AAS 23-258

THE PERTURBED HODOGRAPH

Paul S. Lane*

The velocity hodograph, as laid out in Richard H. Battin's "An Introduction to the Mathematics and Methods of Astrodynamics" provides an interesting frame for observing influences on orbital motion. The nondimensional nature of the frame provides insight into the effects on eccentricity, Flight Path Angle, and True Anomaly or apsidal shift. In this paper, gravitational influences such as J2 and three body motion are explored in the hodographic frame. Assessments performed in this frame may be useful for determining optimal, or near optimal, solutions for spacecraft maneuver plans.

INTRODUCTION

This study investigates the hodograph, which is typically used to visually depict Keplerian motion as velocity vectors that trace out a circular orbits in velocity space. However, for the perturbed motion considered, the resulting non-circular hodographs provide unique insight into orbital motion. The presented results have direct applications for spacecraft in Earth and Lunar orbits.

There are several different Hodograph types typically used in orbital mechanics. Some of the most common types are used to investigate velocity, acceleration, and angular momentum. In the 1968 paper "Orbital Information Derived from its Hodograph," J. B. Eads Jr[1]. demonstrates that simple Keplerian motion produces a circular vector terminus trace in an inertial frame. In the formulation found in "An Introduction to the Mathematics and Methods of Astrodynamics" by Richard H. Battin[2], the velocity vector (**V**) is multiplied by the orbital angular momentum magnitude (h) and divided by the mass parameter (μ) of the central body to produce a nondimensional velocity vector (h**V**/μ). The result is that the terminus produces a circle centered on the Unity Point (1,0) in the rotating frame. Figure 1a shows a typical Keplerian orbit, with the velocity vector in the Local Vertical Local Horizontal (LVLH) rotating frame. In Battin's Hodograph the velocity vector can also be seen in the frame (Figure 1b). The radius of the nondimensional velocity terminus trace represents the eccentricity (e) of the orbit. Other orbital characteristics, such as true anomaly (θ), flight path angle (γ), apoapsis, and periapsis are also represented on the hodograph. When the orbital motion is perturbed the hodograph shape is no longer strictly a circle, and the effects of the associated perturbations can be seen in the trace.

* Visiting Vehicle Officer, Johnson Space Center, Houston TX, paul.s.lane@nasa.gov, KBR, Inc. employee

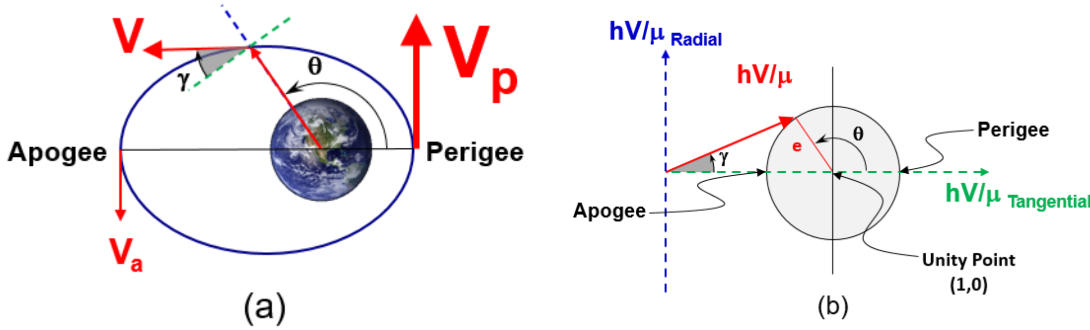

Figure 1. Typical Keplerian Elliptical Orbit and Hodograph in the LVLH Reference Frame.

In this analysis assessments are provided using the "Whole Orbit" and "Localized" methods. The Whole Orbit method plots one or more complete orbit against a reference Keplerian orbit to illustrate differences. The Localized method assesses changes in the curvature locally to determine how and when the perturbing influences effect the motion. By stringing a series of localized assessments together, boundaries between influence regions can be observed. So, Whole Orbit assessments are useful for an initial evaluation of orbital perturbations, while Localized assessments provide boundaries of influence and further insight into the perturbations.

The following examples illustrate how the hodograph may be used to gain insight into orbital parameters for Low Earth Orbits (LEO) and for Near Rectilinear Halo Orbits (NRHOs). The LEO examples have many immediate applications, while the NRHO examples are applicable to trajectories such as those being considered for future lunar exploration missions. First, the hodograph is shown to generally be noncircular for LEOs. Next, this study examines how observing the behavior of true anomaly, argument of perigee, eccentricity in hodographs provides insight into the nature of the departure from Keplerian motion. Throughout this paper, the techniques of Whole Orbit and Localized analysis will be demonstrated.

LEO PERTURBED ORBIT

In this first example a LEO orbit is propagated with an 8x8 gravity model (see Appendix A for details.) The drag terms are sufficiently small as to not dominate the motion. This means that J2 (i.e. the oblateness of the Earth) will be the dominant perturbation for this assessment.

Basic LEO Perturbed Hodograph Motion

Figures 2 and 3 show two traces of 500x400 km LEO trajectories with the apsis aligned with the Equator (i.e. Argument of Perigee (ω) set to 0 deg.) In Figure 2 the True Anomaly (θ) is set to 0 deg at time t_0, while the plot in Figure 3 $\theta = 90$ deg at t_0.

In these figures, the beginning of the orbit, Perigee, and Apogee are indicated. The motion of the Hodograph trace is counterclockwise, and the distance between the Unity Point and the Hodograph trace (blue) is equal to the osculating eccentricity. A time history plot of the osculating eccentricity is also provided in the upper right of each figure. These plots show the typical "duck foot" pattern of a J2 osculation, as expected. The Perigee Point occurs when the Hodograph trace crosses the y-axis, going from negative to positive, while the Apogee Point occurs when the trace crosses the y-axis going from positive to negative. These figures demonstrate that the LEO Hodograph trace is no longer a simple circle. A reference circle is shown, which represents a Keplerian orbit with an eccentricity of 0.008. By comparing the Hodograph trace to the reference Keplerian circle, an initial Whole Orbit assessment shows that the θ = 90 deg orbit may be more representative of Keplerian motion (i.e. more shaped like a circle), but neither orbit appears to produce a simple circle. The rounded triangular shape shows that this motion is organized around three distinct axes and that the orientation of these axes is related to where the orbit is in the osculation phase. Note that in Figure 2, the apsidal events (Apogee and Perigee) occur at extremal points on the eccentricity plot, but in Figure 3 they are shifted. This can also be seen in how the rounded triangle is slightly rotated.

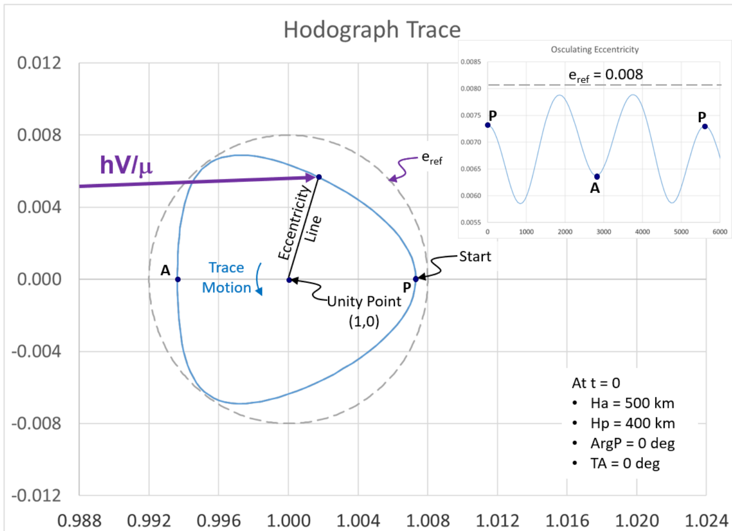

Figure 2. LEO trace Hodographs (True Anomaly = 0; Argument of Perigee = 0).

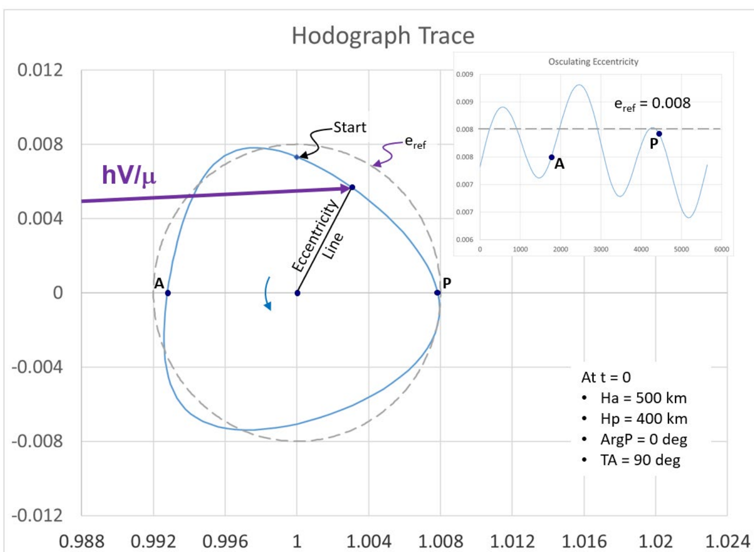

Figure 3. LEO trace Hodographs (True Anomaly = 90; Argument of Perigee = 0).

Argument of Perigee Effects

This example shows the effect that changing the Argument of Perigee has on the orientation of the Hodograph trace. Intuition might indicate that for every degree that the Argument of Perigee changes, there is a 1 deg change in the orientation of the hodograph, but Figure 4 shows that this is not the case. Instead, it appears that the change is ~3 to 2.

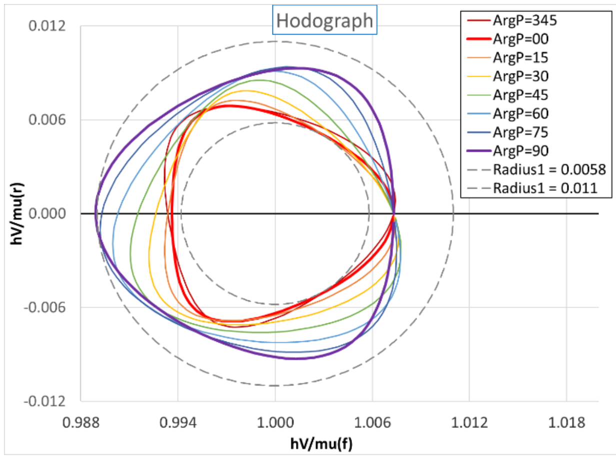

Figure 4. Hodograph Trace for Varied Argument of Perigee.

Eccentricity Effects

This example is a continuation of the previous two examples. Figure 5 shows a series of orbits with decreasing eccentricity (Hp=400 km, ArgP =0). As the height of apogee (Ha) decreases, the hodograph moves from a rounded triangle to an arrowhead and then to a double circle. Getting to the double circle means that the hodograph has progressed to the "peanut" shaped LEO orbit, which is characterized by having two apogees and two perigees. In the final trace (Ha=410) one can see that the trace crosses the y-axis (i.e. zero radial velocity line) twice to the left and twice to the right of the Unity Point.

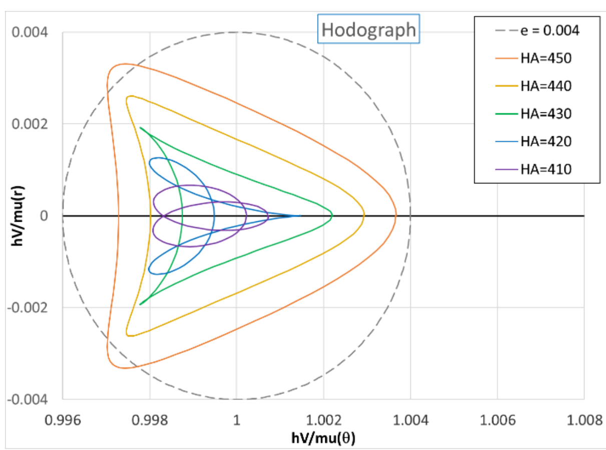

Figure 5. Hodograph Trace for Varied Eccentricity.

Center of Curvature (CoC) Trace for Localized Assessments

By determining the center of curvature at each point in the orbit (reference Appendix B below for details on how this is calculated) a Localized method of analysis can be used to follow the trend of the perturbing influences. The next example focuses on the behavior of LEO orbital motion using this Localized method. Figure 6 shows the perturbed orbit, along with a circle representative for the curvature of the trace at perigee. As the trace moves counterclockwise around the Unity Point, the CoC shifts down and to the left. At point 2 the Hodograph trace has reached the maximum flatness for this segment of the orbit. When the radius of curvature (i.e. distance between the Hodograph trace and the CoC) reaches a maximum, the Hodograph trace has reached a local maximum flatness. Likewise, if the radius of curvature reaches a minimum, the Hodograph trace has reached a local maximum roundness. However, in order to be compliant with Keplerian motion, the CoC must lie on the Unity Point. So, CoC departure from the Unity Point is indicative of perturbing influences.

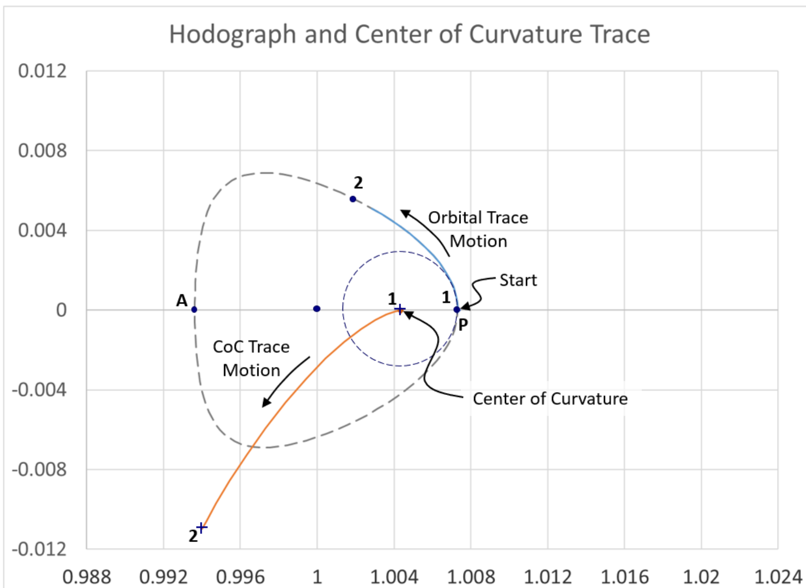

Figure 6. Hodograph and Resulting Center of Curvature (CoC) Trace.

The full CoC traces of the θ = 0 deg & θ = 90 deg orbits can be seen in Figures 7 and 8 (Hodograph Trace is blue and the CoC trace is orange.) Note that while the hodograph trace makes one revolution around the Unity Point, the CoC trace makes two revolutions (*Points of interest, labeled 1-6, are provided on the Hodograph and CoC traces to help the reader follow the corresponding effects*.) Also, the CoC trace has three maximum and three minimum CoC values, with each maximum having a corresponding minimum somewhat aligned with it (e.g. in Figure 7 note that point 1, which represents a local maximum roundness, and point 4, which represents a local maximum flatness, lie on the same line extending outward from the Unity Point.) Finally, note that the CoC trace never goes through the Unity Point. This means that every portion of the orbit is perturbed and never follows Keplerian motion.

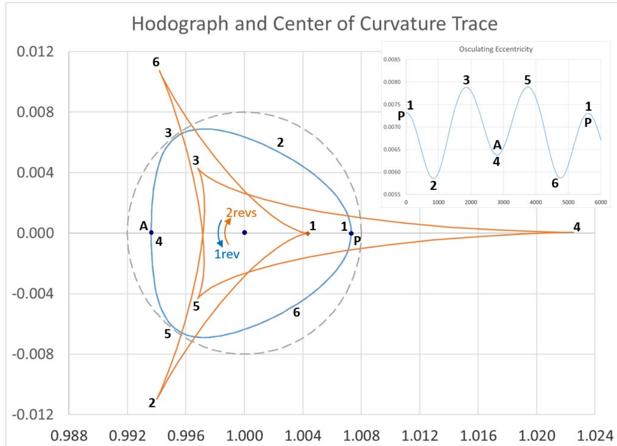

Figure 7. One Orbit Hodograph and CoC Traces (True Anomaly = 0; Argument of Perigee = 0).

True Anomaly Effects

In this example, using Figures 7 and 8, both the reference Keplerian orbit circle and the CoC traces are provided, so both Whole Orbit and Localized assessments can be performed. Defining the orbit with different true anomaly values yields a slightly different orientation of the hodograph and results in a moderate shift in the orbital osculation phase. Though the height of apogee and the height of perigee are the same, the hodograph traces are slightly shifted. Figure 7 shows the orbital trace and CoC trace of an orbit with the apsis defined along the equator ($\theta(t_0)$=0 deg), and it yields a symmetric trace about the Y-axis. However, by defining the orbit with the true anomaly of 90 deg ($\theta(t_0)$=90 deg) the hodograph and CoC traces are rotated in a clockwise direction, as previously noted. However, with the CoC trace included the amount of shift in the osculation phase can be more accurately measured. In Figure 7, point 4 was on the y-axis, but in Figure 8 it is rotated ~12 deg about the Unity Point.

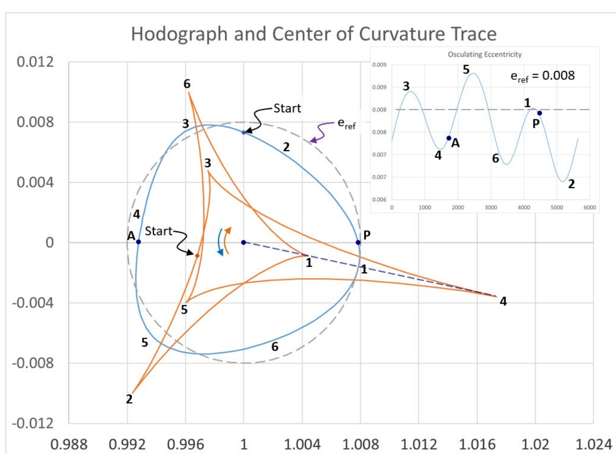

Figure 8. One Orbit Hodograph and CoC Traces (True Anomaly = 90; Argument of Perigee = 0).

Argument of Perigee Effects using Localized Analysis

A similar type of shift can be seen for the previous LEO example if instead θ is held constant and the Argument of Perigee (ω) is varied. Figure 9 shows that the hodograph trace rotates clockwise as the Argument of Perigee increases from zero. Note that the ω = 0 deg trace (Red) and the ω = 90 deg trace (Violet) are pointing in opposite directions. Also, it can be seen that while ω was rotated 90 deg, the CoC trace only rotated ~60 deg, with the lower-left lobe of the Hodograph trace rotating to the left side of the plot. This rotation can be seen in both the Hodograph plot (Figure 4) and the CoC trace (Figure 9), however the CoC trace allows for a more accurate assessment.

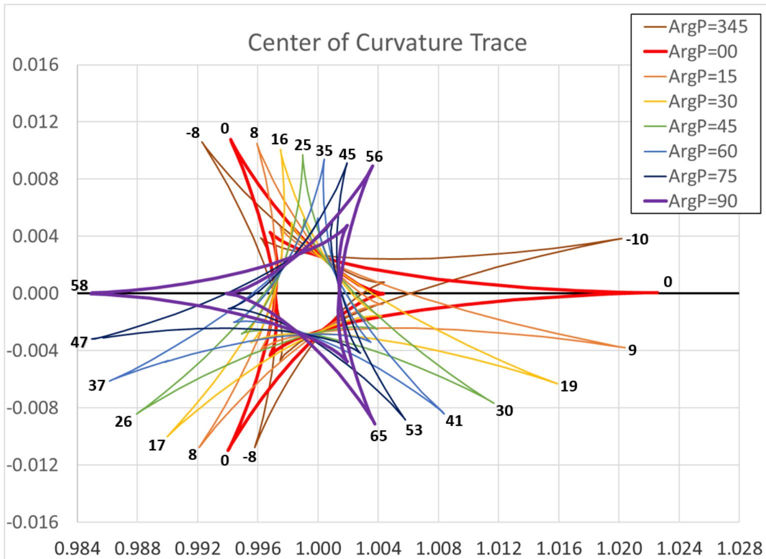

Figure 9. CoC Traces with Varied Argument of Perigee from -15 to 90 deg.

Also, in the CoC trace plot, it can be seen that none of the orbits shown have a CoC trace going through the Unity Point in the center. This shows that this family of LEO orbits do not follow Keplerian motion and are perturbed continuously. However, there are certain points in the ω = 90 deg case that approach the circular hodograph and appear to be closer to Keplerian motion than the closest ω = 0 deg point.

Eccentricity Effects using Localized Analysis

Through a progression of eccentricities, one can see that the curvature of apogee passage in the examples using the 500x400 km orbits (e.g. Figures 2 & 3) is concave (i.e. bending outward from the Unity Point). As the eccentricity decreases the curvature becomes convex (i.e. bending inward toward the Unity Point, as in Figure 10). This transition, occurring around apogee passage, from concave to convex means that the CoC moves rightward out to infinity and then reappears to the left. So, it never passes through the Unity Point, which means that it does not pass through Keplerian motion. Also, as the eccentricity decreases, the apogee and perigee points move toward the Unity point, but the apogee point moves faster and crosses over.

Figure 10 shows the CoC trace next to the associated Hodograph trace. From this series of traces, the effects of eccentricity on the CoC can be seen. As the eccentricity of the orbit goes toward a circular orbit, the CoC trace goes through very large swings initially, as the shape of the Hodograph shifts from the rounded triangle to arrowhead, and then to a double circle.

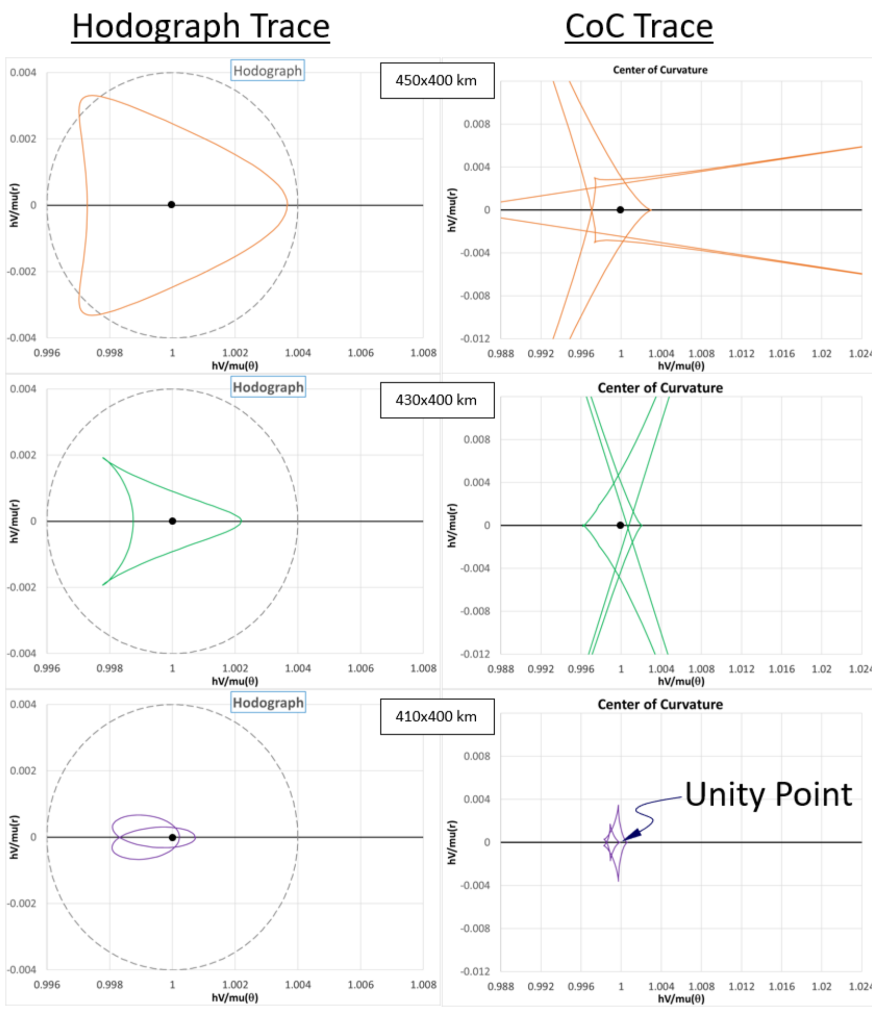

Figure 10. Hodograph and CoC Traces for Different LEO Eccentricities.

Figure 11 is an isolation of the apogee passage of the 430x400 km orbit and shows the elements of the convex Hodograph. The CoC (orange) is outside the Hodograph tract (green.)

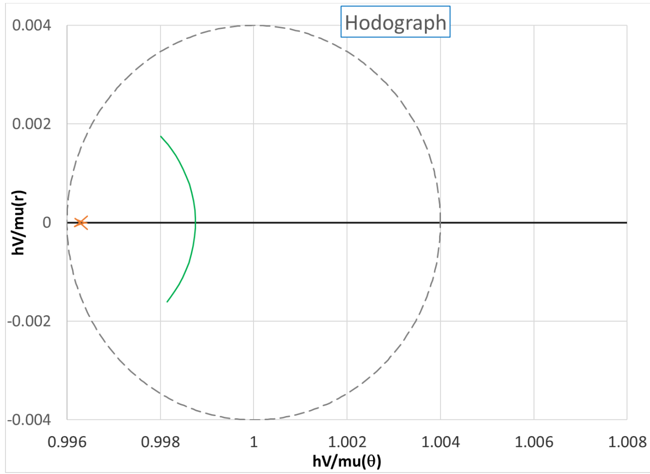

Figure 11. Convex Hodograph Motion (430x400 km Orbit).

Also, Figure 12 is provided to show that the CoC for the 410x400 km orbit doesn't quite pass through the Unit Point, though it appears there may be a special case, with sufficiently low eccentricity that could achieve it. Looking at this progression in reverse, there may also be some high values of eccentricity that result in Keplerian motion. However, Keplerian motion for LEO orbits is not generally expected.

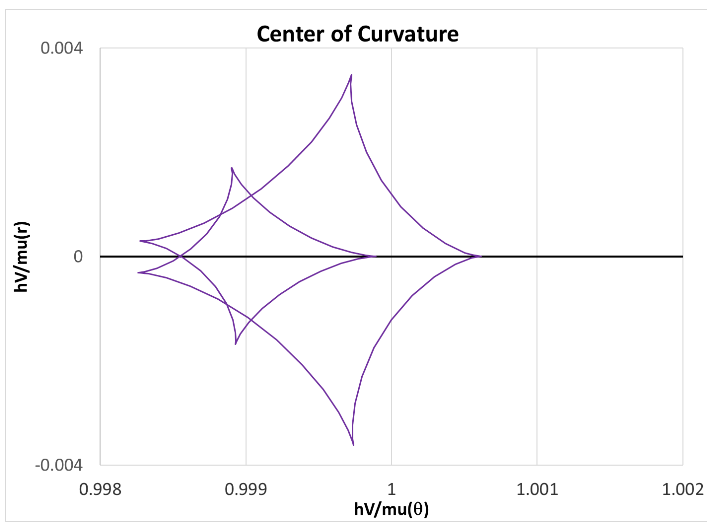

Figure 12. Convex Hodograph Motion (430x400 km Orbit).

NRHO PERTURBED ORBIT

The following section turns to the NRHO perturbed orbit. As will be shown, the NRHO has three distinct regions of motion whose behavior vary depending on their relation to the lunar Sphere of Influence (SOI).

Basic NRHO Perturbed Hodograph Motion

For the NRHO assessment, the orbit considered is that baseline orbit for the Gateway lunar space station. Like the LEO cases, the hodograph provides insight into the orbital motion of this type of orbit. The orbital period is ~6.5 days, with a 9:2 lunar synodic resonance (9 lunar revolutions in 2 lunar synodic months.) The apolune radius for this orbit varies up to 71,000 km and perilune radius is approximately 3,500 km (also noted in Appendix A.) In Figure 13, the full nondimensional velocity vector (violet) can be seen, with the origin of the frame at the center of the y-axis. Apolune and perilune are clearly identified on the hodograph trace, and the motion is counterclockwise as was seen for the LEO assessments. The start and end of this trace was picked somewhat randomly because this is not a closed orbit, and part of this analysis is to show the shift between subsequent orbits.

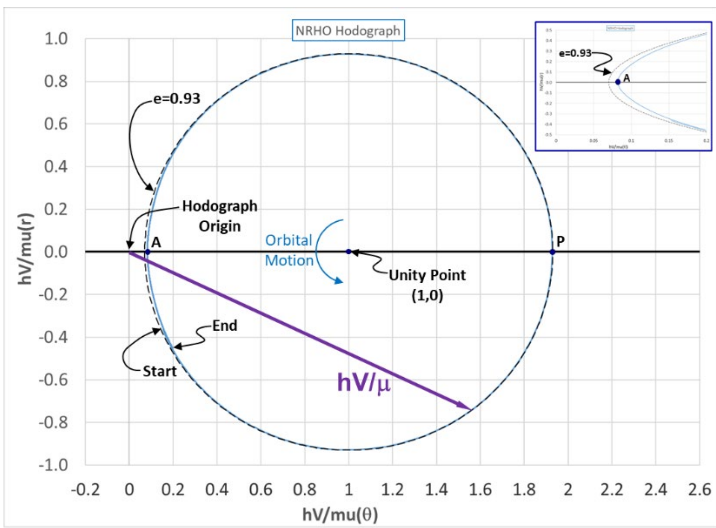

Figure 13. NRHO Hodograph Elements.

A reference circle is included to represent a Keplerian orbit with eccentricity of 0.93, to support a Whole Orbit assessment. One can see that there is a good match around perilune, but there is a clear divergence near apolune. See the exploded view of the apolune passage in the upper right corner of the figure. This indicates that Keplerian motion is clearly not seen at apolune but may be seen at perilune for the chosen NRHO. The divergence from the Keplerian orbit is clear, but a localized assessment is needed to determine the boundaries of the influences involved.

In Figure 14, the Localized analysis shows that the CoC forms a star shape centered on the Unity point. To understand the perturbing effects, the following plots will show the portions of the Hodograph along with the associated CoC trace.

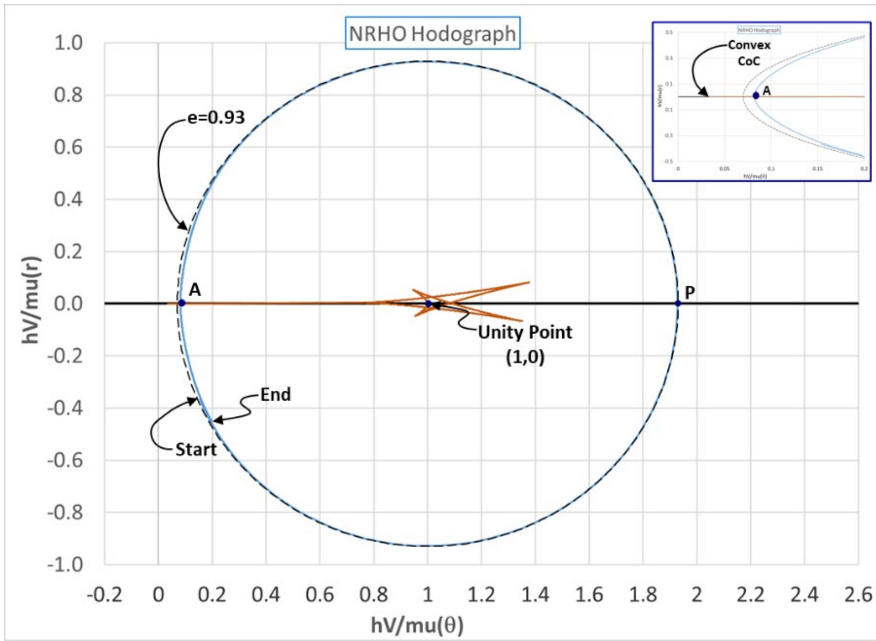

Figure 14. NRHO Hodograph and CoC Trace.

In Figure 15, the perilune passage portion of the Hodograph and the associated CoC (red) is shown. Most notable here is that the moment of perilune passage is the same moment that the CoC trace goes through the Unity Point. This provides further proof that Keplerian motion is seen at perilune. As the two traces move from the A point to the B point, the motion is reminiscent of an athlete performing the hammer throw. As a side note, if one were to draw a line from the Unity point to the CoC trace, it would only lie on top of the Eccentricity line (line from the Unity point to the Hodograph trace) at Perilune. Prior to Perilune it would lead and after Perilune it would trail. For this analysis this Region of the orbit will be referred to as the "Rock Region."

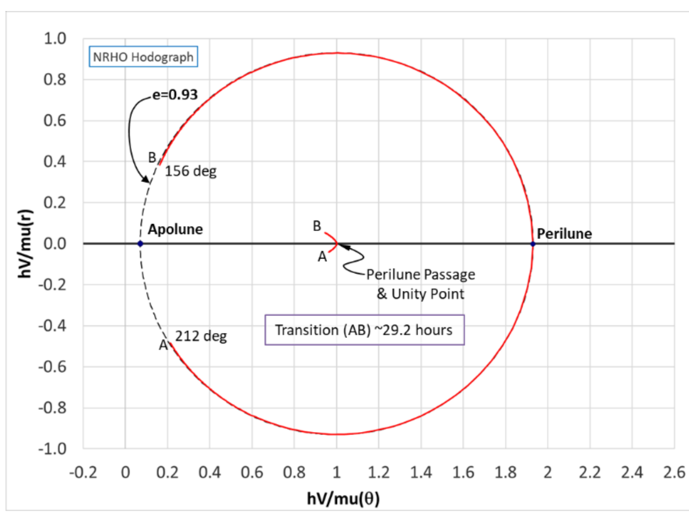

Figure 15. NRHO Perilune Passage "The Rock Region".

In Figure 16, the Hodograph motion has clearly departed from the reference circle (i.e. the gap between the Keplerian reference circle and the segments BC & EA' is clearly seen), and the CoC trace shows that there is a significant angular perturbation (i.e. perturbed along the Y-axis). Interestingly, in the paper "Orbit Maintenance Burn Details for Spacecraft in a Near Rectilinear Halo Orbit,"[3] the optimal locations for performing orbital corrections were determined to be around True Anomaly of 160 deg and 200 deg, which happens to be the same region where the CoC traces cross the Y-axis. Apolune and Perilune are also considered optimal points for correction burns, but due to sensitivity of the solutions, Perilune is not a practical option. As can be seen in Figures 15 and 17, the CoC for Apolune and Perilune also lie generally on the Y-axis. This segment of the orbit will be referred to as the "Paper Region."

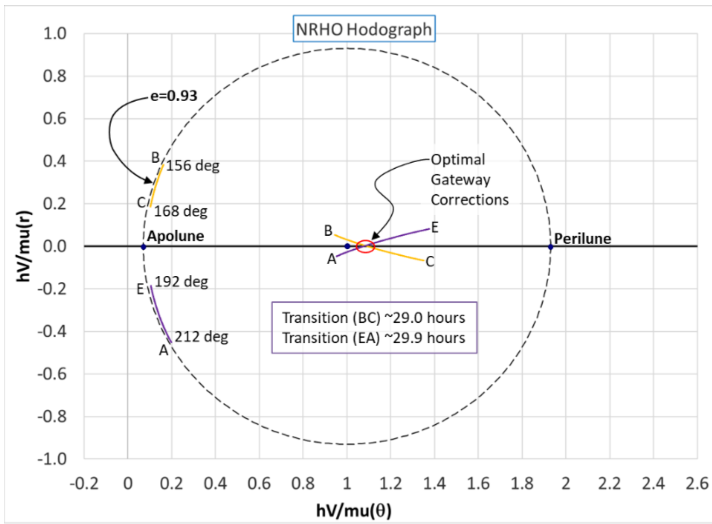

Figure 16. NRHO Transition "The Paper Region".

The top portion of this "Paper Region" appears to be consistent with the edge of the Lunar Sphere of Influence. The Lunar SOI can be estimated using:

$$r_{SOI} \approx 0.9431\ a(m/M) = 62{,}425 \text{ km} \tag{1}$$

Where,

Earth Mass: M = 5.9724 E+24 kg

Moon Mass: *m* = 7.346 E+22 kg

Lunar Semimajor Axis: a = 384,400 km

At Point C, the radius is 61,325 km and at Point E the radius is 61,545 km. So, it appears that the Localized assessment can be used to estimate the transition between Earth and Lunar influences.

Figure 17 shows the apolune passage segment of the orbit, also called the "Scissors Region" in this analysis. The CoC trace points the Scissors to the left, with the handles at points C & E. Note the large swings in the CoC, which seem to indicate how much small influences can affect the shape. Also note that most of the perturbing effect is to shift the CoC along the Y-axis. This CoC shape is somewhat like the LEO perturbation during Perigee passage for the Argument of Perigee = 90 deg case (see Figure 9.)

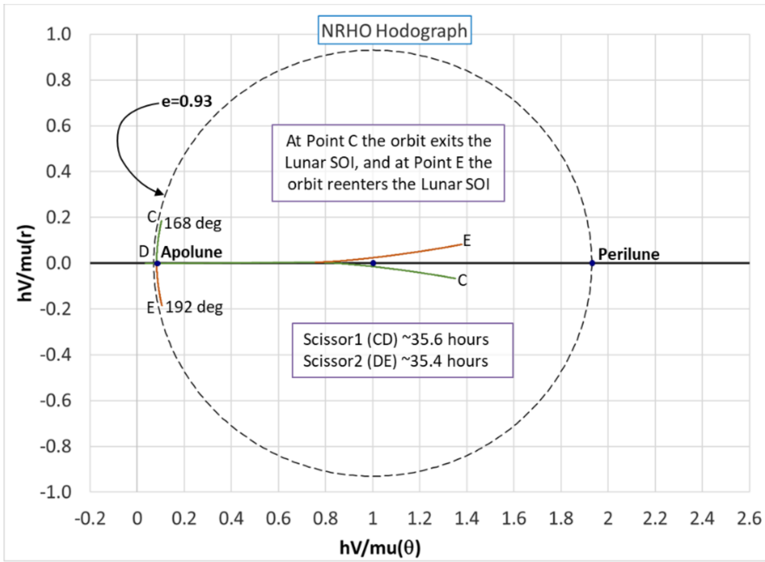

Figure 17. NRHO Apolune Passage "The Scissors Region".

In Figure 18, the different segments are presented with a color code. In the upper right, a time history trace of the eccentricity is shown. The "duck foot" pattern is seen around apolune, but the perilune passage comes to a point. Also, note that the eccentricity at perilune of subsequent orbits is not at a constant eccentricity. This is because the NRHO is a semi-stable open orbit, so the orbital parameters are somewhat bounded, but they do not tend to repeat.

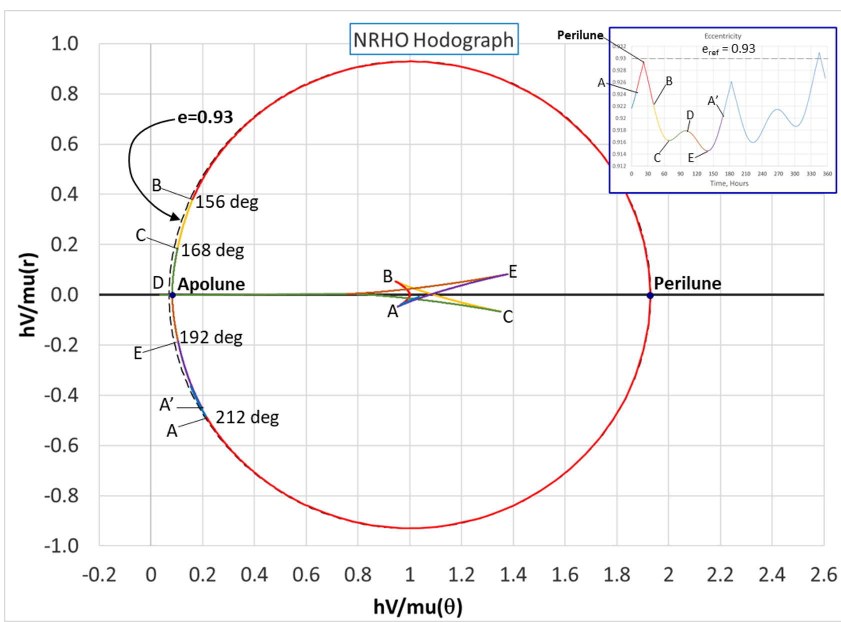

Figure 18. NRHO Hodograph and CoC Traces.

Table 1 shows the duration of each CoC segment. It is interesting to note that the one Rock orbital segment and the two Paper orbital segments have roughly the same durations. Also, the two sides of the Scissors segment have roughly the same duration. So, it appears that there is a three-part symmetry inside the Lunar SOI and a two-part symmetry outside.

Table 1. Segments Durations.

Segment	Duration (Hours)	Comment
A-B	29.2	Rock
B-C	29.0	Paper
C-D	35.6	Scissors
D-E	35.4	Scissors
E-A'	29.9	Paper

CONCLUSIONS

This paper demonstrated how hodographic analysis may be used to gain insight into LEO and NRHO trajectories. Both Whole Orbit and Localized assessments were presented to study the behavior of orbital motion with regard to specific orbital parameters. Further investigation of these results would prove beneficial in understanding the effects of perturbations and specifically how those perturbations can predict orbital parameters for non-Keplerian motion.

In the LEO analysis, it was shown that Keplerian motion is not expected for these orbits. As the orbit approaches circular, the perturbations dominate, producing a second apsis, and Keplerian motion is not typically seen. It was also seen that changing the true anomaly had a small effect on the shift in the orbital osculation phase, while shifting the argument of perigee produced a larger shift. Intuition may have indicated that the argument of perigee change would shift the phase one for one, but this analysis shows that the 90 deg change resulted in only a 58 deg phase shift, which is a ~2 to 3 relationship.

In the NRHO analysis, it was shown that the motion for the planned Gateway NRHO has three distinct regions of motion (*in this paper referred to as Rock, Paper, and Scissors*), two of which are within the Lunar SOI. The Rock region of motion tended to stay closer to Keplerian motion, with the orbit meeting the Keplerian motion criteria at perilune. In the Paper region of motion, there seems to be an optimal region for orbital corrections, which is marked by smaller radial offsets of the CoC. The Scissors region of motion contains the apolune. The Rock and Paper segments were shown to have similar durations, and the two segments of the scissors motion were shown to be near symmetric in shape and time.

By using both the Whole Orbit and Localized assessments, boundaries of influence were shown. Also, it appears that if Keplerian motion is seen, it tends to be associated with periapsis.

APPENDIX A: PROPAGATION DETAILS

Gravity Models

The gravity models used for propagation are as follows:

Earth Model: Grace Gravity Model 02C 8x8; μ_e = 398600.44 KM^3/S^2

Moon Model: GSFC Preliminary GRAIL Gravity Model 50x50; μ_e = 1738.00 KM^3/S^2

Initial LEO State Vector Parameters

The state vector used for the LEO study was initialized with the following parameters:

T0 = 2023-12-17 10:35:12 GMT

I=90 deg

RAAN=0

Mass = 337.998 kg

Area = 40004.0 cm2

SRP = 0

Cd = 2

NRHO Ephemeris Information

The details of the NRHO ephemeris used in this paper is from the Gateway Baseline, which is consistent with the one used in Reference 3. The apolune radius for this orbit varies up to 71,000 km and perilune radius is approximately 3,500 km. It has a 9:2 resonance with the lunar synodic period, resulting in a ~6.5-day lunar orbit. Also, this NRHO is derived from the L2 family, with Apolune to the lunar south.

APPENDIX B: CENTER OF CURVATURE COMPUTATION METHOD

To determine the Center of Curvature (CoC), select three consecutive data points. In Figure 19, the midpoint of each line segment can be determined by averaging the coordinates of each line segment end points:

$$\underline{\text{AB}}: MP_1 = \frac{X2+X1}{2},\ \frac{Y2+Y1}{2} \tag{2}$$

$$\underline{\text{BC}}: MP_2 = \frac{X3+X2}{2},\ \frac{Y3+Y2}{2} \tag{3}$$

Also, the slope of each line segment is determined by the following "rise over run" equations:

$$\underline{\text{AB}}: M_1 = \frac{Y2-Y1}{X2-X1} \tag{4}$$

$$\underline{\text{BC}}; M_2 = \frac{Y3-Y2}{X3-X2} \tag{5}$$

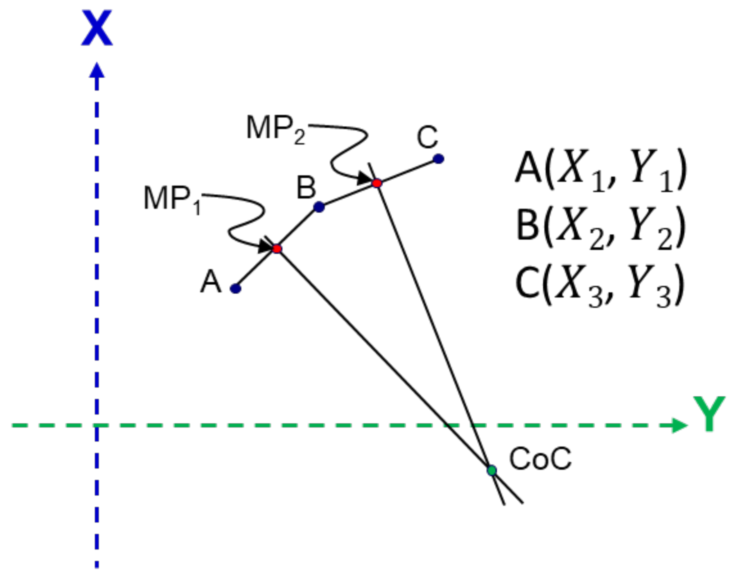

Figure 19. Center of Curvature Determination.

To determine the intersection of the lines orthogonal to the initial line segments, the constants for these lines must be determined. The negative inverse of line segment AB slope (M_1) is the slope of orthogonal Line1 (i.e. line segment MP_1 to CoC). Likewise, the negative inverse of the line segment BC slope (M_2) is the slope of orthogonal Line2.

$$\text{Orthogonal Slope of AB: } F_1 = \frac{-1}{M1} \tag{6}$$

$$\text{Orthogonal Slope of BC: } F_2 = \frac{-1}{M2} \tag{7}$$

So, the equations for these orthogonal lines are:

$$Y_1 = F_1 \ X + K_1 \tag{8}$$

$$Y_2 = F_2 \ X + K_2 \tag{9}$$

Where the K terms are found by inputting the midpoint coordinates MP_i(x,y),

$$K_1 = -F_1 \ MP_1(\text{x}) + MP_1(\text{y}) \tag{10}$$

$$K_2 = -F_2 \ MP_2(\text{x}) + MP_2(\text{y}) \tag{11}$$

Figure 20 shows that the first term of Equations (10) & (11) is the slope times the x off-set of the midpoint, and the second term is the y off-set of the midpoint.

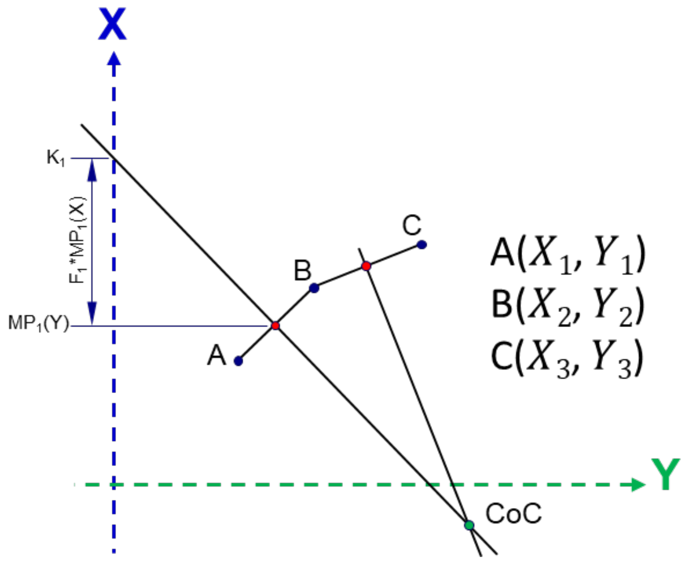

Figure 20. Illustration of the Y-Intercept Solution.

Solve for the intersection by setting $Y_1 = Y_2$ from Equations (8) & (9):

$$F_1\ X\ + K_1 = F_2\ X\ + K_2 \tag{12}$$

Solving for X yields:

$$X = \frac{K_1 - K_2}{F_1 - F_2} \tag{13}$$

Once the X ordinate of the intersection has been determined, the Y ordinate can be determined by plugging the X value into Equations (8) & (9). As a quality check, use both equations to confirm that they yield the same result. Note that there is a singularity in the case that $F_1 = F_2$, so error handling may be needed.

ACKNOWLEDGMENTS

The author would like to thank Joseph Frisbee, Diane Davis, Julie Read, Patrick Casey, and Nathaniel Ylitalo for insightful discussions, generous guidance, and continual support.

REFERENCES

[1] J. B. Eades, Jr., “Orbit Information Derived From Its Hodograph”, Goddard Space Flight Center, July 1968.

[2] Richard H. Battin, “An Introduction to the Mathematics and Methods of Astrodynamics, Revised Edition”, American Institute of Aeronautics and Astronautics Education Series, 1987, pp. 126-128.

[3] Diane C. Davis, Stephen T. Scheuerle, Dale A. Williams, Frederick S. Miguel, Emily M. Zimovan-Spreen, and Kathleen C. Howell, “Orbit Maintenance Burn Details For Spacecraft in a Near Rectilinear Halo Orbit”, July 2022.